UNITED STATES DEPARTMENT OF THE INTERIOR
GEOLOGICAL SURVEY

A Practical, Low-noise Coil System for Magnetotellurics

by

W. D. Stanley and Richard D. Tinkler

Open-File Report 83-85

1983

A Practical, Low-noise Coil System for Magnetotellurics
U.S. Geological Survey Open-file Report No. 83-85

by

William D. Stanley and Richard D. Tinkler
Box 25046, MS 964, Denver, CO 80225

Introduction

Magnetotellurics is a geophysical technique which was developed by Cagnaird (1953) and Tikhonov (1950) and later refined by other scientists worldwide. The technique is a method of electromagnetic sounding of the Earth and is based upon the skin depth effect in conductive media. The electric and magnetic fields arising from natural sources are measured at the surface of the earth over broad frequency bands. An excellent review of the technique is provided in the paper by Vozoff (1972). The sources of the natural fields are found in two basic mechanisms. At frequencies above a few hertz, most of the energy arises from lightning in thunderstorm belts around the equatorial regions. This energy is propagated in a wave-guide formed by the earth-ionospheric cavity. Energy levels are higher at fundamental modes for this cavity, but sufficient energy exists over most of the audio range to be useful for sounding at these frequencies, in which case the technique is generally referred to as audio-magnetotellurics or AMT. At frequencies lower than audio, and in general below 1 Hz, the source of naturally occuring electromagnetic energy is found in ionospheric currents. Current systems flowing in the ionosphere generate EM waves which can be used in sounding of the earth. These fields generate a relatively complete spectrum of electromagnetic energy that extends from around 1 Hz to periods of one day. Figure 1 shows an amplitude spectrum characteristic of both the ionospheric and lightning sources, covering a frequency range from 0.0001 Hz to 1000 Hz. It can be seen that there is a minimum in signal levels that occurs at about 1 Hz, in the gap between the two sources, and that signal level increases with a decrease in frequency.

It is typically necessary for most magnetotelluric surveys to require MT measurements over a frequency range of .001 to 100 Hz. Because of the nature of the spectrum shown in figure 1, a very sensitive magnetometer is required for the aquisition of data for frequencies from .01 Hz upward. In the early days of the method, large induction coils with mechanical chopper amplifiers were used (Hopkins, 1965) for MT sounding. These coils consisted of long solenoids with many thousands of turns of wire, cored with high magnetic permeability Ni-Fe alloy material. The weight of a typical coil was about 35-60 kg, with three such coils being required to measure the Cartesian components of the magnetic fields needed for the MT soundings. For low-frequency measurements only, fluxgate or alkali vapor magnetometers have been employed for the magnetic field recording. For audio-magnetotelluric measurements, efficient ferrite cored induction coils have been employed. Starting in 1974 (Fredrick and others, 1974) magnetometers based upon superconducting effects were taken from the laboratory into the field and used for magnetotelluric measurements. These magnetometers, called **SQUIDS** (superconducting quantum interference devices), have very low noise levels and are compact and light weight. A typical SQUID magnetometer has intrinsic noise levels of less than .0001 nT and with a small helium Dewar can weigh as

little as 15 kg for a three component system, as opposed to the 100-180 kg of the older induction coil systems. Air core induction sensors have also been used to measure the magnetic fields (Campbell, 1969), although horizontal magnetic component measurements are difficult to make with large diameter air-core coils in a field environment.

SQUID magnetometers were largely accepted as the optimum magnetometer for magnetotellurics after several commercial manufacturers began to offer improved versions of early systems. Cost of a three component SQUID magnetometer, however, has increased from about $18,000 in 1977 to $35,000 or more in 1981. A commercially manufactured induction coil system can be obtained for about $20,000, a figure that still represents a major cost in construction of an MT system.

In an attempt to provide an inexpensive and practical magnetometer for magnetotellurics, the USGS has developed an induction coil and pre-amp system which attempts to meet the following objectives:

(1) low in cost, with a materials cost of $1500 (1981 prices) for a three component system,
(2) light weight, with a weight of 15.5 kg per coil, as opposed to the 35-60 kg of previous induction coils used in MT,
(3) broad bandwidth, with a useable frequency response up to 1000 Hz,
(4) ease of construction, such that a coil-preamp system can be built with a minimum of equipment and technical ability, and
(5) reliability, such that all components are readily available and unreliable or high failure rate components have been eliminated.

The induction coil sensors are similar to those described by Hopkins (1965), Hill and Bostick (1962), and Karmann (1975) except they have been optimized for ease of construction, low weight, and signal to noise ratio. The low noise chopper amplifiers were derived from designs developed by Becker (1980) with major redesigns effected to lower noise and size, and increase reliability of the amplifiers. The induction coils consist of a 152 cm (60 in) long, 1.9 cm (0.75 in) square cross-section permalloy core with 48,000 turns of 28 gauge copper wire wound on 8 separate sections. Weight of the completed 152 cm (60 in) coils is 15.5 kg and the outer housings have a diameter of 10.2 cm (4 in).

The coil amplifiers use a full-floating, bridge chopper input based upon integrated circuit transistor switches. Chopped or modulated signals are amplified by a dual-differential amplifier coupled with active filters to control the bandwidth of the modulated signals. Demodulation is accomplished using another integrated circuit transistor switch package. Additional low-pass active filtering and passive low-pass filtering is done to attenuate switching transients and match the amplifier response to the coil transfer function to provide linearization.

Coil Components

The major coil components are shown in figure 2. The laminated permalloy core consists of 10 layers of .159 cm (0.0625 in) thickness permalloy (80% Fe, 20% Ni) material laid in brick fashion to avoid gaps in the 76 cm (30 in) and 38 cm (15 in) long pieces. The core material has a relative permeability of

35,000. The laminated core is tightly contained in an acrylic tube by wrapping the core with high density, closed cell foam sheet before insertion in the tube. The coil is wound on eight standard, magnet-wire spools, which have been bored out so that they fit tightly on an acrylic tube containing the laminated core. The connection is made between the eight separate windings by reducing flame welding of the copper magnet wire ends together. Soldering is avoided because of the generation of thermocouple voltages at the junctions of soldered copper wires. The connected wire spools are fastened onto the core tubing by aluminum clamps which have set screws to jam the spools together. The assembled core and winding assembly is contained in an outer housing made of 0.635 cm (0.25 in) wall thickness, 7.62 cm (3 in) I.D. PVC tubing. End caps made from standard plastic pipe fittings close off the ends of the housing to provide a water tight sensor. To provide additional ruggedness and thermal and vibration insulation, an outer protective cover and foam sheet padding was added.

Coil Specifications

The amplitude response of the 152 cm (60 in) coil is shown in figure 3a. A single pole response is evident up to about 30 Hz, shown by the 1/f slope. Above 30 Hz the response curve begins to flatten due to eddy currents losses in the coil core. At 700 Hz the first resonance of the coil is observed, with a rapid fall-off in response above 700 Hz. This very high resonant frequency results from the low distributed capacitance obtained by the nature of construction involving winding the coil on eight separate coil forms and by not coating the windings with lacquer. The eddy current amplitude reduction above 30 Hz is not a problem, since the MT measurements have to be corrected for the coil transfer function in any case. The eddy current flattening could be moved up in frequency by using thinner laminations in the coil core, but it has been stated by Bozorth (1942) that the amount of magnetic domain noise (Barkhausen noise) in a magnetic material is proportional to the number of longitudinal divisions. Thus, there seems to be a disadvantage in using thinner laminations, since all that would be achieved would be to move the eddy current flattening upward in frequency. The 0.159 cm (0.0625 in) thickness material is easy to obtain, and when laminated has a great deal of mechanical strength. A solid bar of permalloy of the correct diameter is much more difficult to obtain. Also, the material must be magnetically annealed in a special furnace after any mechanical working such as cutting or machining. Annealing furnaces long enough to handle a 152 cm (60 in) rod are not as common as ones that will handle the maximum 76 cm (30 in) pieces of this design. For these reasons, the use of 0.159 cm (0.0625 in) material cut into pieces as described below seems to be a practical, if not optimum solution to the core problem.

The coil, with 48000 turns of 28 gauge copper wire, has a resistance of 1720 ohms. The inductance is about 650 Henries and the capacitance is about 20 picofarad (pf). As shown in figure 3a the output at 1 Hz is 136 uvolt/nT. The coil resistance provides a noise floor of Johnson noise at about 5.2 nvolt/$\sqrt{Hz}$. The coils described in Hill and Bostick (1961) have larger diameter wire (22 gauge) and more weight (41 kg), with a winding resistance of 330 ohms, giving rise to a Johnson noise of only about 2.3 nvolt/$\sqrt{Hz}$. The larger Johnson noise in the coils of this report seems to be a good tradeoff for the factor of three decrease in weight achieved by our design.

Coil Construction

The objective of this section is to provide a readily reproducible procedure for construction of the coils described in this report. It is hoped that the detail is sufficient to allow anyone interested to construct the coils with a minimum of difficulty. [A set of data sheets for all components used in the coil and amplifier construction can be obtained by writing the first author (W. D. S.). However, readers are encouraged to contact the authors if the documentation is not clear or if they have comments or questions on procedures.] With this in mind, we follow a step by step construction description.

Core assembly

The core material was obtained from AD-VANCE Magnetics, Inc.*, 625 Monroe Street, Rochester, Indiana. A 76 cm (30 in) x 152 cm (60 in) sheet of 0.159 cm (0.0625 in) AD-MU-80 was supplied cut into 60 pieces 1.9 cm (0.75 in) x 76 cm (30 in) and 40 pieces 1.9 cm (0.75 in). This consists of enough material for three 60" long coils. The pieces were magnetically annealed by the vendor after cutting. Each lamination was coated with a single thickness of mylar tape so that the laminations were electrically isolated from each other to reduce eddy currents. The laminations were then assembled in brick pattern fashion using two 76 cm (30 in) pieces end to end, then the next lamination having a 38 cm (15 in) piece-76 cm (30 in) piece-38 cm (15 in) piece, and so forth. This procedure, of course, avoids having gaps in the material which would cause mechanical problems, and fringing of the magnetic field lines from inside the core to outside, reducing the effective permeability of the core. Assembly was accomplished with the aid of a jig made from (2.54 cm (1 in) O.D. aluminum channel stock with 0.159 cm (1/16 in) wall thickness. A 152 cm (60 in) piece of this material provides a trough into which 10 laminations can be assembled. Once the laminations are assembled and aligned in the channel, a square rod can be used to push the asembled core slowly out one end of the channel. After about 8 cm of the core has been pushed from the channel, a C-clamp can be used to squeeze the laminations tightly together, so that fiberglass tape can be wrapped around the laminations to keep them secured. The very end of the core should also be thus secured as well as at each 8 cm interval and at each 38 cm (15 in) length (to coincide with the joints in the core laminations). The material will be slightly warped due to the annealing process, so there will be noticeable gaps of a few hundredths of millimeter along the core, even when the material has been clamped and tightly wrapped every 8 cm. This is not a problem, since the final step in construction of the core is to coat the top and bottom of the core with two-part epoxy, which is forced into the laminations with a paddle. A more complete coating and bonding of the core could be achieved by placing the core in a form constructed so that the entire core could be flooded with a lacquer or epoxy and allowed to dry. The procedure used here was a first trial at producing an easily constructed core, with the view in mind of modifying the construction if the first trial was not successful. However, after two years' testing and

* The use of trade names in this report is for specifications documentations only and does not represent endorsement by the U.S. Geological Survey. Other vendors of this and other products described herein are available.

use in the field, the first effort seems to be highly satisfactory, but readers may be able to improve on our construction and are encouraged to do so.

Once the core laminations have been taped and glued, the core is ready to be inserted into the coil center tube. In order to achieve a tight fit into the center tube, the core is wrapped with high density, closed cell polyethelene foam sheet, which is secured by wrapping the foam with flat, braided nylon cord (used normally for tieing electrical wiring together). Foam sheet of .64 cm (.25 in) thickness should be cut so it may be wrapped around the core with about a .5 cm (.2 in) gap. The single, cut sheet of foam is then secured by wrapping with nylon cord in spiral fashion, with loops about 3-6 cm apart. After the first attempt at tieing down the foam, the wrapped core can be inserted into the center tube. The center tube is clear acrylic tube stock with 3.8 cm (1.5 in) O.D. and 3.2 cm (1.25 in) I. D., which has been cut to a length of 155 cm (61 in). If the inserted core is too loose, then the foam should be rewrapped to allow it to expand. Of course, if it is too tight, then the nylon wrapping will have to be tightened.

Coil winding

Construction of the coil itself has been simplified by the use of standard 7.6 cm (3 in) diameter, 10.2 cm (4 in) long magnet wire spools, which are available from Groggins Plastics, RFD #2, Box 121, Fincastle, Virginia. The plastic spools are wound with 6000 turns each of #28 gauge copper magnet wire with Formvar coating, although any standard magnet wire coating of any temperature range will suffice. The 6000 turns of #28 wire amounts to about 1000 linear meters (3300 ft). The wire can be obtained pre-wound in footage amounts from Magnet Wire Services, Mountain View, California. Spooled wire supplied by this company may be specified to have the bottom end of the wire left projecting through the side of the spool, so that the wound spools can be connected together in series to make the induction coil. Winding by turns provides a more consistent calibration for each finished coil, since wire stretch makes winding by footage somewhat more variable, but even then the effects on calibration are quite small (less than 2 percent between two coils from effects of winding alone). If the spools are to be wound on a lathe, as we have done, then the details of our procedure may be of assistance.

A simple aluminum arbor was constructed to allow the spool to be chucked into a lathe. This arbor is shown in figure 4; a bolt and washer on the outside end allow the spool to be loosened so that it may be rotated by hand to start the wire on the spool. With a turns counter installed or by using a footage counter, the winding is initiated by laying down at least two layers of wire in an uncrossed, perfect level wind. After the first two neat layers are completed, using a lathe speed of about 100 rpm, the speed of winding can be increased to about 250 rpm and the wire should then be laid down in a smooth, but not perfectly layered fashion. The only criterion is that the windings should be evenly distributed, so that there are no large lumps left when the spool is completed. The wire can be spooled directly from 4.54 kg (10 lb) spools of magnet wire which contain about 6100 m (20,000 ft), or enough for about 6 spools. Before the wire is put on the spools, five holes should be drilled on each end of the spool. A drilling template is shown in figure 5 which will facilite this task. The four outer holes are at quadrant

points just below the lip of the spool and a single inner hole is drilled below one of the outer holes and just above the spool axis level. The bottom end of the wire should project about 20 cm through the latter hole. The projecting end should be taped to the spool during the winding and boring out of the spool. The outer holes are used for passing the outer connecting wires and for connecting the spools mechanically.

Once the spooling of the wire has been completed, both ends should be secured on the face of the spool and the windings should be wrapped with tape to keep them from unwinding. The centers of the spools now have to be bored out to 3.8 cm (1.5 in) approximately, with the actual diameter taken from the exact piece of tubing used to contain the permalloy core. Dimension of the bore should be such that the spool have a hand-press fit on the acrylic tubing. This can best be done using blank spools for test boring. The boring of the wound spools is facilitated with the aid of a collet made from 7.6 cm (3 in) I.D. 0.635 cm (0.25 in) thick aluminum tubing as shown in figure 6. The tubing has been cut to a length of 10.2 cm (4 in), scribed through two-thirds of the wall thickness at 8 or 9 points, and then cut through completely on the last scribe. The wound coil can be inserted into the collet, which can then in turn be chucked into the lathe so that the spool can be bored out, but with protection for the wire. The spools can be wound after boring out the centers but we wanted to have a procedure to also work with spools pre-wound by a commercial supplier.

Coil and Core Assembly

All of the completed spools should be checked for a resistance of about 215 ohms. A clamp constructed of aluminum stock as shown in figure 7 should be placed on the core tubing at a point necessary to center the eight spools on the tube. The first spool is placed up against the clamp and then the second spool is placed on the core tube about 8 cm from the first. If the fit of the spools on the core tube is a little loose, a strip of tape can be placed down the center of the spool bore to make a tight fit. We found this procedure to be necessary, although more careful machine work might avoid the need for the tape. The bottom end of the second spool can be joined to the top end of the first to form a series connection. About 8 cm of spare wire should be left and the connection made by welding the twisted ends together with an oxy-propane or oxy-hydrogen torch. Welding of the wire avoids the thermocouple voltages occurring when two copper wires are soldered.

We secured the spools to each other by first sticking down the connecting wire between the spools with calking putty. The putty secured the spools together when they were pressed in conjunction so that all of the spools could be assembled on the core. Once all eight spools had been placed on the core and connected, the other end clamp was installed and 2-56 brass machine screws and nuts were used in the two of the outer holes indicated on figure 5 to fasten the spools together. As a last step, cyanoacrylate adhesive was flooded into the cracks between the spools and the end clamp set screws tightened to keep the spools jammed together.

The top wire from the last spool installed may now be brought along through the pre-drilled holes in each spool and secured to the end of the coil from the first spool installed with a clamp or tape. The ends of the #28 coil wire can be connected to the external world with #20 or #22 untinned copper

wire with the aid of copper binding posts or by welding them as we have done. Again, soldering should be avoided because of thermocouple voltage generation.

A final step in the coil assembly is the installation of 0.64 cm (0.25 in) foam sheet on each of the spools. The foam is cut long enough to just meet when wrapped around a spool and then secured with Ty-Wrap or similar material. The foam is cut to fit inside the spool rims as shown in figure 8. The foam protects the wire, keeps it in place, ensures that the coil assembly fits snugly into its housing, and provides thermal and vibration insulation.

Final Assembly

The completed coil-core assembly is placed in the 7.6 cm (3 in) I.D. PVC tubing, which has been cut to a length of 155 cm (61 in). End caps can be constructed of a 8.9 cm (3.5 in) diameter disk of plastic, nylon, or phenolic as shown in figure 9 or machined from standard 7.6 cm (3in) threaded plastic pipe plugs (one of each is shown in figure 9). The center of the caps is bored out to 3.8 cm (1.5 in) so that the end of the core tube will be supported when the end caps are in place. Once the end caps are installed in the outer housing, they can be drilled and tapped through the housing. A watertight passageway should be provided through the end cap for the coil leads to pass to the pre-amp. After the end caps have been installed, the coil is essentially complete, but an additional cover can be used for further vibrational and thermal isolation. This is accomplished by wrapping the coil in 0.64 cm (0.25 in) foam sheet and securing with nylon cord, and then inserting the whole assembly into a 0.159 cm (0.062 in) wall, 10.2 cm (4 in) O.D. PVC tube. This procedure adds only about 1 kg to the overall weight and is probably valuable from the standpoint of protection and thermal isolation. An electrostatic shield can be added to the coil by putting strips of 5 cm (2 in) aluminum tape along its length, separating the strips by about 1.5 mm. The strips can be electrically connected by wrapping buss wire around them at one end of the coil. Standard, slip-on plastic pipe caps can be used to close off the outer protective coil cover. This provides an additional water barrier if the caps are coated with silicone rubber before installation. The coil is now complete and ready for calibration and testing.

Coil Calibration and Testing

The coil system described in this report was calibrated using two independent methods. The first check of coil sensistivity and frequency response was done in a large Helmholtz coil system, consisting of 2m diameter coils with a separation of 2 m. It was expected this this would be only a rough calibration and was done to check the design parameters. After this initial calibration, which provided numbers that were in reasonable agreement with those predicted from calculations, an additional calibration was done by placing the sensor coils in a long solenoid. The solenoid consisted of 3 m of 25.4 cm (10 in) diameter PVC pipe wrapped with 25 turns of no. 22 gauge copper wire. The wire was wrapped in uniform, spiral fashion from one end to the other. This winding was used to impress a magnetic field on the sensor coil located in the solenoid. A sine wave generator driving an operational amplifier type power supply provided sine-wave currents of up to one ampere to the calibration winding. A precision 1 k ohm resistor in series with the

calibration coil provided a 1 volt/milliampere reference signal for an HP 3582 digital spectrum analyzer. Amplitude and phase responses were obtained at a large number of discrete frequencies by using the transfer function determination provided by feeding the voltage across the 1 k ohm resistor into the reference input and the output of the sensor coil (or combined coil-preamp) into the other channel of the two-channel spectrum analyzer. The calibration from the Helmholtz coils agreed very well with the calibration using the solenoid. The solenoid method is very rapid and the field inside solenoid is easily calculated from the known turns and input current, so that this method can be used even under field conditions to check sensor calibrations.

Coil Amplifier

Because of the extremely low voltage levels at the coil output, a very high quality amplifier is required to amplify these voltages to useable levels. The need for a very low noise amplifier is evident when it is considered that magnetic signal levels of 0.001 nanoTesla (nT) are frequently encountered in the frequency band around 1 Hz, as shown in figure 1. With a coil sensitivity of 136 uvolt/nTHz, this means that the coil output will be 136 nanovolt (nv) for a 0.001 nT signal at 1 Hz. The same coil output will be obtained with a 1 nT magnetic signal at 0.001 Hz, so this is not an unreasonable signal level to consider in designing a coil amplifier. The Johnson or thermal noise floor of the coil winding is about 5.2 $nVHz^{-1/2}$ as mentioned above; therefore, a coil amplifier should have a noise level no larger than this and should have a flat noise characteristic at low frequencies, rather than a large 1/f noise slope. Earlier coil amplifier designs used components which were much higher in noise than those available currently. Because of this, the amplifiers required transformer input to raise coil voltages and match input impedances. The amplifier described in this report takes advantage of recent developments in FET (field-effect-transistor) and CMOS (complementary-metallic-oxide-semiconductor) technology.

Theory of Amplifier Operation

A block diagram of the chopper amplifer used with the coil system is shown in figure 10. All semiconductor devices exhibit various types of noise that can be referenced to their input or "front end". The advantages of using a chopper amplifier is that it minimizes the 1/f component of the noise. This type of noise is inversely proportional to frequency and usually is the dominant noise component for frequencies below 10 Hz. For a complete discussion of noise sources in electronic amplifiers, the reader is referred to Motchenbacher and Fitchen (1973).

The key to operation of a chopper amplifier is conversion of the signal to be amplified to an AC signal with a frequency significantly higher (at least two decades) than the corner frequency of the 1/f noise of the actual amplifier section before the signal is fed to the amplifier section. After amplification the 1/f noise is superimposed on the modulated (chopped) version of the original information signal. If the modulated (chopped) signal contains only frequencies higher than the 1/f noise corner, the 1/f noise can be removed by a high pass filter whose corner is less than the modulation frequency, but greater than the 1/f corner frequency.

History of Amplifier Development

The final amplifier described in this report is actually the fourth generation developed during 1981. Description of the historical development may add insight into the reasons for details of the final design. The first chopper amplifier completed was based upon a single pole, single throw input chopper with a JFET differential amplifier. The input chopper switch consisted of an n-channel, low-noise JFET and the demodulator consisted of a low-pass filter alone. The amplifier negated the 1/f noise component, but was quite noisy over the whole frequency band because of a poor AC amplifier design and the limitations of the simple chopper-demodulator design.

The second attempt consisted of constructing the chopper amplifier described in Becker (1980), with the assistance of Dr. Francis Bostick, Jr., University of Texas, Austin, who provided circuit boards and a great deal of information on this design. Becker's design used a full bridge (commutating) input chopper consisting of four MOSFET transistors and associated logic. The demodulator consisted of three MOSFET transistors designed to reconstruct the modulated signal and to short the reconstructed signal during small time slices in order to kill chopper transients occuring during switching periods. It also employed a feedback type amplifier consisting of a three op-amp (operational amplifier) instrumentation amplifier with an unmatched, extremely low noise JFET pair in the feedback. Complex logic was needed to drive the chopper and demodulator. The completed amplifier had good noise characteristics of less than 10 nV/ Hz from 10 Hz down to at least .1 Hz. The commutating chopper worked very well, except that the use of MOSFETs was found to be very troublesome, due to their high failure rate during handling of the amplifier. Keeping resistors across the inputs and using body grounds on technicians did not seem to cure the problem completely in the low humidity, high static environment of Denver, Colorado. The differential amplifier stage required tedious matching of the input transistors and for this reason, the Teledyne 2N6550 transistors specified for the original design by Becker were replaced with a matched pair, a Siliconix 2N5517.

The third amplifier to be built was a slightly modified version of the Becker amplifier. In this design, the MOSFET chopper and demodulator transistors were replaced by p-channel JFET transistors to improve reliability. In addition, the transient suppression switching at the demodulator was left out, as were several gain control stages. The board area was reduced by using miniature capacitors and placing resistors on end. Also, Texas Instruments TL072 dual, low-noise op-amps were used exclusively. The integrated circuit voltage regulators used in Becker's design were found to be a source of output noise and they were eliminated with the use of a low noise DC/DC convertor which supplied the +15 and -15 volts from a 12 volt battery. An output buffer, DC offset adjust, and passive output low-pass filter were added to the design. The finished amplifer performed well, having about $7 nV/\sqrt{Hz}^{-1/2}$ noise levels from 10 Hz to 0.1 Hz, and appearing to be very reliable. The only drawback for this version (and also a characteristic of the Becker version) was positive clipping of input signals caused by the breakover of the input JFETs (or MOSFETs also) with signals voltages greater than 0.5 volts. Normal MT signals would never provide coil outputs above this level, but 60 Hz power line fields produced voltages higher than this in he areas where the coil system was being tested near Denver. The clipping of AC signals varying in amplitude caused large amplitude DC offsets in the

output. This problem only existed at our test areas near Denver and was not encountered during field surveys in the summer of 1981 in the Pacific Northwest, when the third version amplifiers were used exclusively. The amplifiiers were contained in 7.6 cm (3 in) x 10.2 cm (4 in) shielded boxes and placed about 2 m from the sensor coils, receiving power from a single 12 volt motorcycle battery. The coil-amplifier system proved extremely reliable and provided excellent MT data when compared with a SQUID magnetometer. The reduction in size of the amplifiers from two 10.2 cm (4 in) x 38 cm (15 in) circuit boards of the Becker design to a much smaller 7.6 cm (3 in) x 10.2 cm (4 in) two-board design made for a more practical field system.

The fourth (and final?) version of the chopper amplifier developed consists of a complete redesign based upon our previous experiences. The concept of a commutating or bridge chopper and double-pole demodulator is the same as in the Becker amplifier, but most of the rest of the design was completely redone. The discrete FET transistors used in the modulator and demodulator have been replaced by integrated circuit CMOS analog switches. The analog switch ICs have built in circuitry to negate the positive side clipping mentioned above, and because of the biasing scheme built into the switch ICs, the input chopper could be operated in a floating configuration, rather than with one side tied to ground as in the Becker and our version three designs. This is quite important as will be demonstrated below. The feedback differential amplifier was replaced by two cascaded differential amplifier stages employing dual, matched JFETs (2N5517, Siliconix) with constant current source biasing. The differential amplifiers are AC coupled to an active two-pole high-pass filter which eliminates the 1/f noise component. A miniature 32 KHz crystal driving two CMOS logic ICs make up the entire digital circuitry necessary for the chopper-demodulator functioning. An optional DC offset circuit was added near the output to facilitate noise measurements and testing. The resulting circuit was contained on a single 3.5" x3.5" circuit board.

This amplifier performed very well, with noise levels between 2 and 3 $nVHz^{-1/2}$ over the frequency band from 0.1 to 10 Hz. Tests comparing this amplifier with the version three amplifier show that the floating input chopper removes a source of noise caused by output cable movement. This cable movement causes a noise voltage which gets fed back into the amplifier input through the ground system. Figure 11 shows an example of movement of an output trunk cable containing both a version three and version four amplifier-coil signal. The effect is seen to be quite large on the version three system (channel 2), but hardly noticeable on the version four system. The improvement is due to better input-output isolation in the version four amplifier.

Version Four Amplifier Operation and Components

A schematic diagram for the amplifier is shown in figure 12, and a printed circuit board layout is shown in figure 13. The coil input comes onto the board at C1, a 10 uf capacitor. In the version three amplifier, it was possible to switch from a 10 uf coil tuning capacitor to a 0.1 uf capacitor. This provided a coil response rolling off at about 1 Hz or 10 Hz, respectively. It was found that using the 10 uf capacitor negated the 60 Hz clipping problem in our test area and appeared to decrease overall output noise when making low frequency recordings; therefore in our field surveys,

the capacitors were switched to 10 uf for measurements below 1 Hz and to 0.1 uf for measurements above 1 Hz. The same option can be implemented on the version four amplifier with an external switch, since mounting holes are provided on the circuit board for both capacitors (or other values). The tuning capacitors also act as a low-pass filter to prevent aliasing of high frequency signals by the input chopper.

The chopper modulator is comprised of a Siliconix DG303CJ dual, single-pole-double-throw analog switch configured as a commutator. The switch configuration is such that coil outputs are switched in polarity on every clock cycle. The choppped or AC signal is fed to the differential amplifier first stage, made up of Q1-Q2, a Siliconix 2N5517 matched JFET pair, and associated parts. The 2N5517 has a noise density of about 2 $nVHz^{-1/2}$ at 2KHz, which is the chopper frequency. Other transistors, such as the Crystallonics 2N6550 used by Becker (1980) have a lower noise density at 2 KHz (about 1 $nVHz^{-1/2}$), but the overall amplifier noise levels will depend as much on transistor matching, differential amplifier common-mode rejection, and bias point stability as much as intrinsic noise density of the individual amplifier transistors. The CR200 (Q5 and Q6) is a 2 ma current regulator diode used to provide the bias point for the 2N5517s and also to act as a high dynamic impedance for improved common mode performance. The differential amplifier stages are AC coupled to aid in biasing and attenuation of the low frequency noise.

The initial amplification is accomplished by the two differential stages, which have an overall gain of about 50. The differential output of the second stage is converted to a single ended signal by the op-amp circuit made up of amplifier A1 and associated resistors. All op-amps are Texas Instrument TL072 dual packages of BIFET design (combined bipolar and FET technology). Extra gain setting resistors are provided by R11 and R9. the overall gain of the coil amplifiers as we are using them is about 2500, but this may be altered with an external switch to utilize resistors R11 and R9 and provide an alternate lower gain value.

After the gain stage and differential to single-ended conversion provided by A1, a voltage follower comprised of A2 buffers the signals to a high-pass filter made up of A3 and associated components. The latter is a two-pole active filter with a corner frequency at 10 Hz. This frequency is high enough to attenuate the 1/f noise from the amplifier and low enough to leave the modulated signal peaks with a relatively square shape.

The demodulator is made up of A4, A5, A6, U3 and associated components. A4 outputs a positive image of the modulated signal, while A5 provides an inverted image of the modulated signal. When the upper pole of the analog switch IC (U3, a Siliconix DG387) is closed, the lower pole is open, passing the positive image of the signal; when the switch positions are reversed, the negative image of the modulated signal is passed. The effect of this operation is to demodulate or reconstruct the original coil signal. The reconstruction is not perfect, due to timing and gain errors in the demodulator, but the defects are in the form of sawtooth discontinuities at the chopper frequency of 2 KHz, which after being buffered by A7, are filtered out by the 9 Hz low-pass filter made up of A8 and associated components. Chopper spikes caused by switched capacitance on the input chopper and demodulator transistors are also highly attenuated at this point.

Following the low pass filter, an optional offset adjust circuit is provided by A9, A10, and A11. This DC offset capability is useful for accurate noise testing with a digital spectrum analyzer, but should be left out for field use, since low frequency noise is increased by the offset circuit. A final buffer, A12, provides a low output impedance and circuit isolation. The chopper drive signals are provided by a 32 KHz miniature crystal oscillator driving a 7 stage divider. The crystal and one gate of the CD4049 hex inverter, with tuning components, form the actual oscillator, and the output of this oscillator is divided by 16 in the CD4024. Phase shifting necessary to properly drive the demodulator in signal reconstruction is provided by three remaining gates of the CD4049 hex inverter.

Amplifier Construction

The circuit board artwork for the component side of the board is shown in figure 14. The components are labeled with their symbolic designation; actual components values may be obtained from figure 12b or from the parts list in Appendix A. The circuit board may be ordered from Astro-Endyne Inc., Boulder, Colorado (job no. 10479) and the remaining parts may be obtained through distributors for the particular parts.

There are seven feed-throughs that have to be installed in the board to carry signals from one side of the board to the other. This is necessary because the circuit boards do not have plated-through holes. The locations of these feed-throughs are shown in figure 14 and should be installed first in constructing the board. The IC sockets should be installed next and should be left elevated above the board about 0.25 in to faciliate soldering the topside pads when necessary. The socket for the CD4049 should be installed after all other components to aid the soldering of other components near the socket.

C16 should be installed next and care should be taken to ensure that the top side solder connections are made. The crystal, U1, can now be soldered in, but care should be taken not to overheat the crystal during soldering. It is not possible to use heat sinks on the crystal leads, because of their length, thus it is necessary to leave the soldering iron on the junction for a minimum time. The crystal leads should be bent at a right angle 1/16" below the case bottom to facilitate soldering to the two parallel solder strips. R23 should now be installed with care taken to make both top side solder connections. The order of installation of the rest of the parts is not critical, but care should be taken to allow access to all top side solder connections.

As noted in the parts list, we are using a low noise DC/DC convertor from Semiconductor Circuits, Inc. as a source of +15 and -15 volts for the amplifier. Other power sources may be substituted as long as the regulation and noise specifications are comparable to those outlined in the data sheet for the convertor we are using (see appendix A). The power source used should be connected to the circuit board with an ammeter in series with the +15 volt supply. Current draw to the board should be about 42 ma from the +15 supply and about 22 ma from the -15 supply. If current draw is considerably larger than these values, components have been installed incorrectly or other problems exist and the board will have to be debugged one section at a time. If the current draw is within range, then the crystal oscillator should be checked for proper operation. The oscillator takes a few seconds to start up

on application of power, but should start reliably. The signal at pin 10 of the CD4049 should be an 8 to 10 volt peak-to-peak sinusoid at a frequency of 32.768 KHz centered around +7.5 volts.

If the oscillator is functioning properly, then an input signal may be applied to the amplifier board for further testing. The input signal should be about 10 Hz and less than 10 mv peak-to-peak amplitude. The output of all stages prior to the demodulator (DG387CJ) should resemble the upper part of figure 15. The output of the demodulator should be similar to that in figure 16 and the output of the low-pass filter should be a very smooth sinusoid. If all signals look correct as described above and the overall gain of the amplifier is between 2500 and 3000, then the amplifier is functioning properly and noise tests can be performed as a final check. We have mounted the amplifier and power supply in a BUD CU-234 11.9 cm (4.7 in) x 9.4 cm (3.7 in) x 5.7 cm x (2.25 in) cast aluminum box (see appendix A for data sheet), and have used a .159 cm (1/16 in) aluminum divider between the circuit board and power supply to reduce pickup of the convertor switching noise by the amplifier. The completed amplifiier is shown in fig. 17.

Amplifier Noise Tests

Shown in figure 18 are photographs of noise tests run with the amplifier (gain of 2500) input shorted. The test was done on an HP 3582 digital spectrum analyzer. The noise is between 2 and 3 $nVHz^{-1/2}$ with the maximum noise at the higher frequencies close to 10 Hz. For lower frequency noise measurements, the output of the shorted amplifier was fed to a band-pass filter used in MT recording and then displayed on a strip-chart recorder. Figure 19 shows such a recording over the frequency band from 0.005 Hz to 0.2 Hz. The peak-to-peak noise over this frequency band is about 35 nv. It has been suggested by Becker (1980) that the peak-to-peak value of such a recording be divided by a "crest factor" of about 8 to arrive at the rms noise voltage. If this is done and we divide by the square root of bandwidth, a value of about 10 $nVHz^{-1/2}$ is obtained for frequencies down to below 0.005 Hz.

The low-pass filter used on the output stage of the chopper amplifier has a corner frequency at 9 Hz as used with the USGS MT system. This filter corner acts to linearize the overall coil-amplifier system response in the 10 Hz region when the coil is tuned with the 0.1 uf capacitor as shown in the overall response curve of figure 20. The corner frequency of the amplifier low-pass filter can be modified by changing the values of R20 and R21 or by changing C10 and C9. The corner frequency of the filter is given by 0.159/RC, where R is R20 or R21 (equal value) and C is C10 or C9 (equal value). The gain of the filter, set by R22 and R23, constrains the filter response to be close to a maximally flat or Butterworth response.

Field Tests of Coil-Amplifier System

In 1981 three coils were constructed, of which two were 152 cm (60 in) long sensors constructed as described above. The third coil was constructed in a different manner and designed to serve as the sensor for the vertical magnetic field. The vertical coil core consisted of 10 laminations of the 0.0625" permalloy material, but was made up on only 76 cm (30 in) pieces, so that the core itself was only 76 cm (30 in) long. The vertical coil was designed to be short so that it could be easily installed into the earth to

reduce vibrational noise. To make up for the loss of sensitivity caused by the shorter core, a different coil winding design was used. For the vertical coil, #32 gauge wire with a total of 60,000 turns on four spools was used. The concentration of magnetic field lines in the core is parabolic from end to end, with the maximun concentration at the center. The bunching of the windings near the core center with the aid of smaller diameter wire on the vertical coil did not completely make up the loss of sensitivity caused by reducing the core length. The vertical coil has a scale factor of 67 nv/nTHz and the winding has a resistance of 5100 ohms, providing a thermal noise figure of 9.2 $nVHz^{-1/2}$. The signal to noise ratios of this design has proven unsatisfactory and two alternate vertical coil designs have also been tested. One of these is a cored coil made up of four separate 76 cm (30 in) cores with two spools with windings of 6000 turns #28 guage wire per core. This coil was not satisfactory because the four separate cores acted as a single core and overall sensitivity was reduced. The vertical coil design, which appears to work well, consists of a large diameter air-core coil made up of 82 turns of #28 gauge wire. This coil consists of standard seismic cable of 100 m length and is designed to be deployed in several configurations, with either its full 100 m perimeter or looped back upon itself one or more times. The air-core coil has a scale factor of 330 uv/nTHz and resistance of 1200 ohms, providing a thermal noise floor of 4.4 $nvHz^{-1/2}$.

The metal cored coils were tested in 1981 by installing them parallel to each other on a center separation of about 2 m. Output of the three coils (two horizontal and the one vertical) and the version three amplifiers were compared over the frequency range of interest in our MT recording system, 0.001 Hz to 12 Hz. Initial testing revealed several problems related to output cabling and grounding considerations between the coil systems and the recording truck, but when these were handled properly, the parallel coil test appeared to be excellent. The coils were then compared with a SQUID magnetometer in actual data recording and processing runs, and these tests showed that the coils provided a striking increase in data quality in the frequency band from 0.1 Hz to 3 Hz and comparable results to the SQUID in the higher and lower frequency bands. The data in these tests was taken simultaneously with both the SQUID and coil systems. Part of the improvement in data quality may be due to the pre-whitening effect of the coils on the input magnetic signals, although we feel a significant part of the improvement is due to actual increase in signal to noise ratio of the coils in comparison to the SQUID at frequencies above 0.1 Hz. Sensitivity of the coil installation to wind noise was as good or better than the SQUID installation under the same conditions. We have completed laboratory noise measurements on three SQUID systems to verify manufacturers specifications, but we do not have adequate simultaneous noise tests on the SQUIDs or coil systems to make quantitative statements about the actual noise of both systems under field conditions as opposed to the theoretical noise figure shown in figure 1.

The coil system of this report has been used with the version three amplifier in performing 30 MT soundings in the Denver area and Pacific Northwest in 1981, and with four additional coils and the version four amplifier to complete 40 soundings in the Great Basin and Pacific Northwest in 1982. The system provided good data and proved very reliable. Simultaneous noise tests of two SQUID systems and two coils in a shielded room used for biomagnetic testing at the National Bureau of Standards, Boulder, Colorado, are planned for the future.

Field Installation of Coils

It has been common practice in using large solenoid sensor coils to bury the coils for a period of time before their use in recording (Hopkins, 1965). The reasons proposed for burying the coils are related to maintainence of thermal and mechanical stability. A number of tests done with the coils of this report indicated to us that the most important factor in noise reduction was to provide a completely level and firm base for the coils to rest upon, and to provide adequate shielding from the wind and sun. If any major portion of the coil was left unsupported or differentially supported, then mechanical stresses set up in the coil caused transient noise to be generated due to settling effects. We found that it was much easier to provide such a competent mechanical support if we did not bury the coils. Major disturbances of the earth in trenching for burial appeared to cause more problems than simply leveling of the surface soil. The coils were placed in very shallow level troughs, with a minimum of ground disturbance incurred, and then covered with a wind and sun shield made of half sections of 10" plastic pipe. Soil was packed up against the sides of the coils before covering with the wind shields. This method of installation proved to be rapid and more reliable than a quick burial and recording sequence. In field tests with a SQUID system in which the SQUID magnetometer was installed with a great deal of care and covered with a wind shield, we found that coils which had been installed as above were as free from wind noise as the SQUID during times of high wind. The coil pre-amplifiers are deployed at a distance of about 2 m from the coils and are all powered from a single, 12 amp-hour motorcycle battery (12 volt). The three coil amplifiers and the two electric field pre-amps are housed in a single, small styrofoam ice chest to provide thermal insolation.

References

Becker, J. D., 1980, A multi-site magnetotelluric system with real time data analysis: Unpub. Ph.D. Thesis, Dept. of Electrical Engineering, University of Texas, Austin.

Cagniard, L., 1953, Basic theory of the magnetotelluric method of geophysical prospecting; Geophysics, no. 18, p. 605-635.

Campbell, W. H.,1969, Induction loop antennas for geomagnetic field variation measurements; ESSA Tech. Rept. ERL 123-ESL6, Dept. of Commerce.

Hill, L. K., and Francis, X. Bostick, Jr., 1962, Micropulsation sensors with laminated mumetal cores; Ph. D. thesis, U. of Texas, Austin.

Hopkins, G. H., Jr., 1965, Instrumentation for geofield measurements; Elec. Eng. Res. Lab Rept. no. 138, U. of Texas, Austin.

Frederick, N. V., W. D. Stanley, J. E. Zimmerman, and R. J. Dinger, 1974, An application of superconducting quantum interference magnetometers to geophysical prospecting; Geoscience Electronics, IEEE, v. Ge-12, no. 3, p. 102-103.

Kawrmann, D. R., 1975, Optimierung des signal/rausch-verhalnisses von induktionsspulenmagnetometern fur die magnetotelluric; Ph. D. thesis, Techical University Carolo-Wilhelmina, Braunschweig.

Motchenbacher, C. D., and F. C. Fitchen, 1973, Low-noise electronic design; Wiley and Sons, New York, 357 p.

Vozoff, K., 1972, The magnetotelluric method in the exploration of sedimentary basins; Geophysics, v. 37, no. 1, . 98-141.

Tikhonov, A. N., 1950, Determination of the electrical characteristics of the deep strata of the Earth's crust; Dokl. Akad. Nauk SSSR, 73(2), 295 pp.

Appendix A, Parts List

C1 10 uf miniature polycarbonate
C2 0.1 uf miniature polycarbonate
C3 0.01 uf disk ceramic
C4 " " "
C5 0.2 uf stacked film (two 0.1 uf in parallel) Siemens supplied
C6 0.1 uf stacked film, Siemens supplied
C7 " " "
C8 " " "
C9 .33 uf "" ""
C10 " " "
C11 .1 uf " " "
C12 10 pf mica
C13 22 pf mica
C14-C17 10 uf electrolytic in parallel with 0.01 uf disk
Q1-Q2 2N5517 Siliconix dual JFET
Q3-Q4 " " "
Q5-Q6 CR200 Siliconix current regulator diodes
U1 DS-VT-200 Seiko 32.768 KHz crystal
U2 Siliconix DG303CJ dual SPDT analog switch IC
U3 Siliconix DG387CJ single SPDT analog switch IC
A1-A12 Texas Instruments TL072 dual low-noise op-amps
U4 RCA CD4024 7-stage binary divider
U5 CD4049 hex inverting buffer
R1 3.32M metal film
R2 " "
R3 6.19K 1% metal film
R4 6.19K 1% metal film
R5 3.32M metal film
R6 " "
R7 5.6K metal film
R8 5.6K metal film
R9 select for alternate gain switching
R10 1.6M
R11 select for alternate gain switching
R12 1.6M
R13 430K metal film
R14 150K metal film
R15 430K metal film
R16 150K metal film
R17 100K metal film
R18 100K metal film
R19 10K metal film
R20 27.4K metal film
R21 " "
R22 22K
R23 10K
R24 68.1K
R25 50K
R26 500 ohm pot (Spectral upright)
R27 50K
R28 10K
R29 10K

R30 22M
R31 1M
R32 100K
R33 100K
R34 10K

Miscellaneous Parts

quantity	
1	16 pin dip socket (wire-wrap or long lead solder type)
3	14 pin dip sockets " " "
6	8 pin dip sockets " " "
1	BUD CU234 aluminum chassis box
1	LD12-15D150 or LA12-15D150 DC/DC convertor from Semiconductor Circuits, Inc.

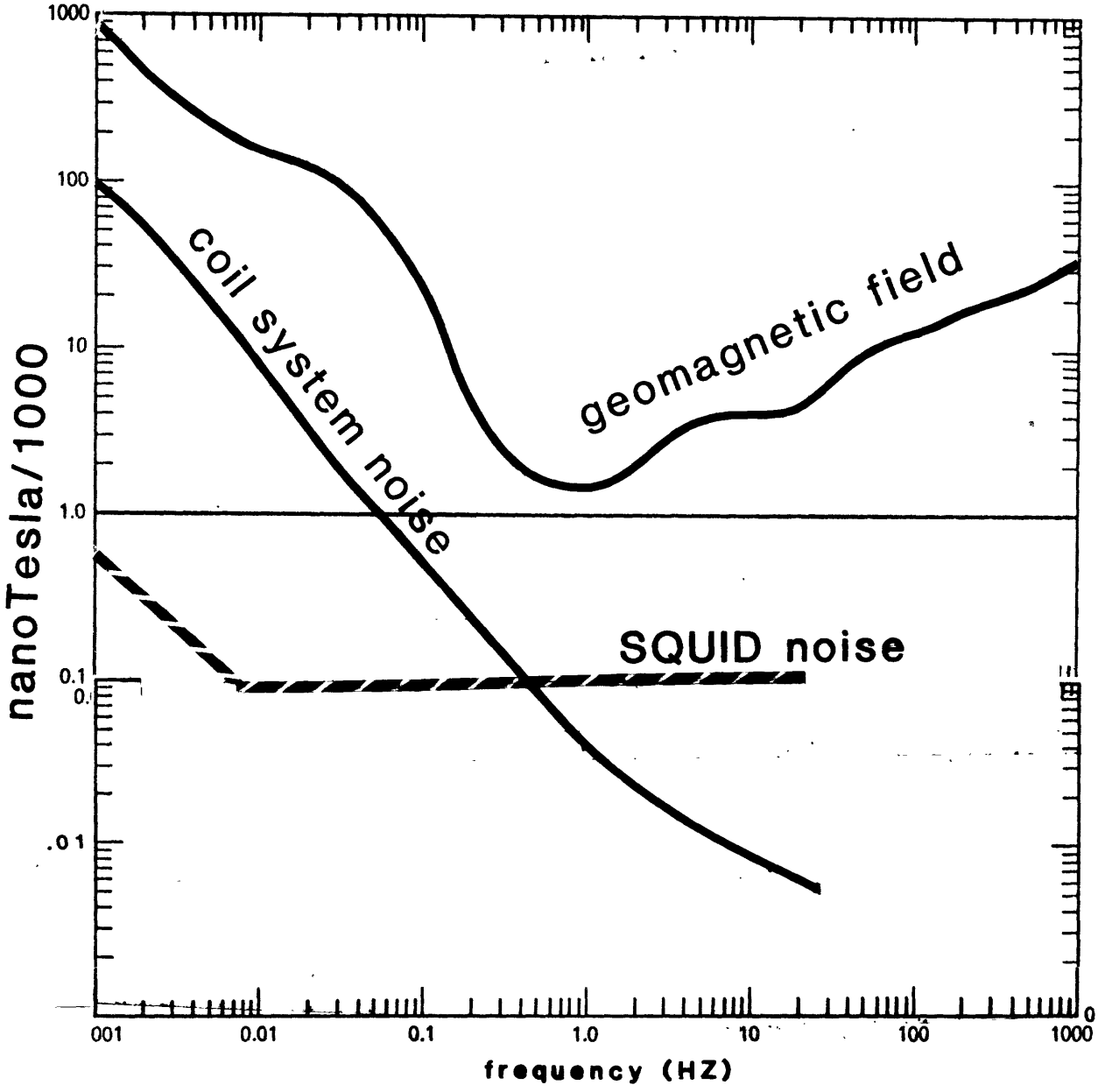

Figure 1.--Spectrum of natural geomagnetic fields and noise spectra for the coil system of this report and a commercial SQUID system. The noise spectrum of the coils system is based upon measured amplifier noise and thermal noise of the coil winding. The noise spectrum of the SQUID was obtained with the sensor shorted, and not with actual magnetic sensor configuration.

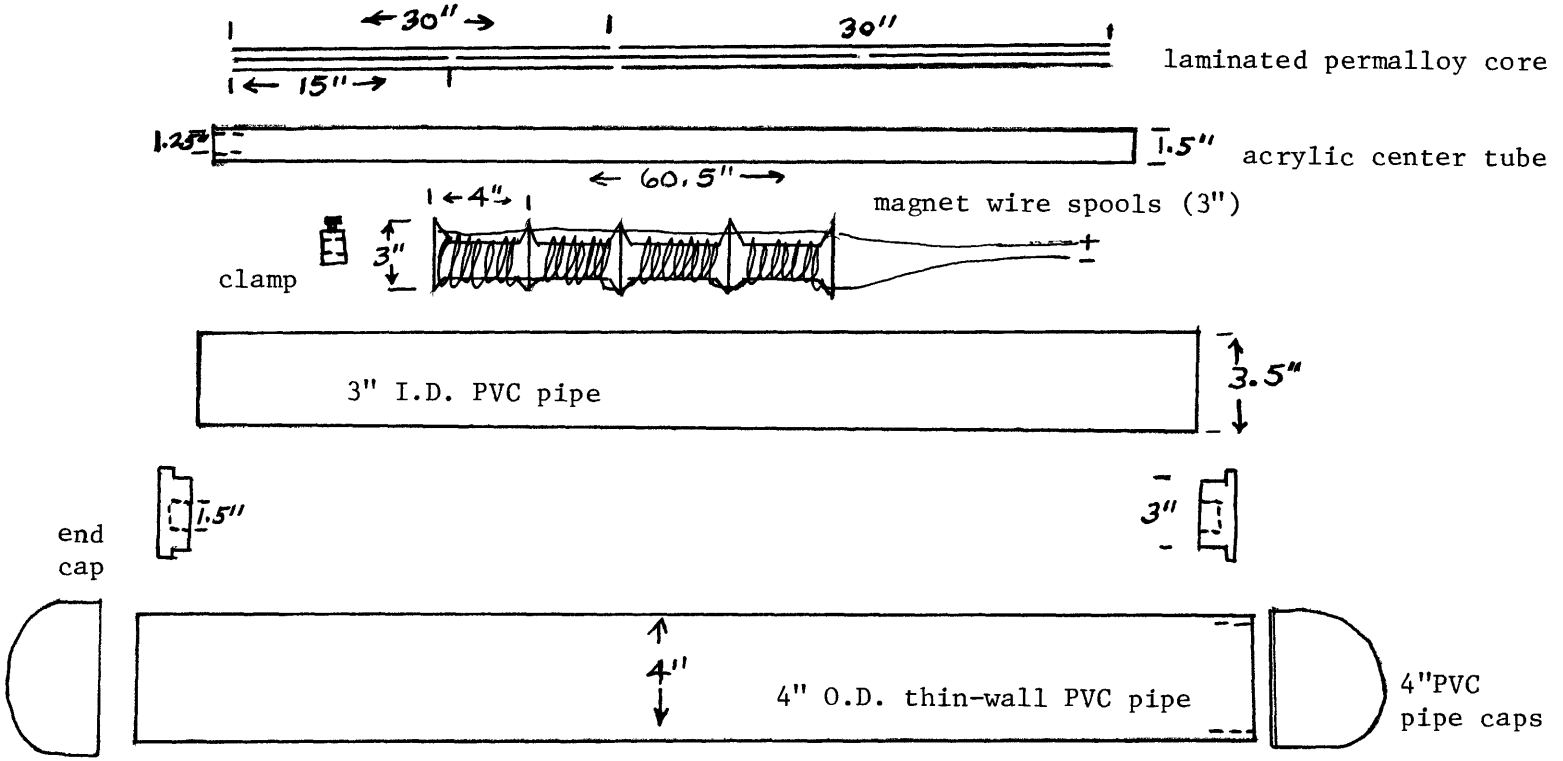

Figure 2.--Diagram of components making up the induction sensor.

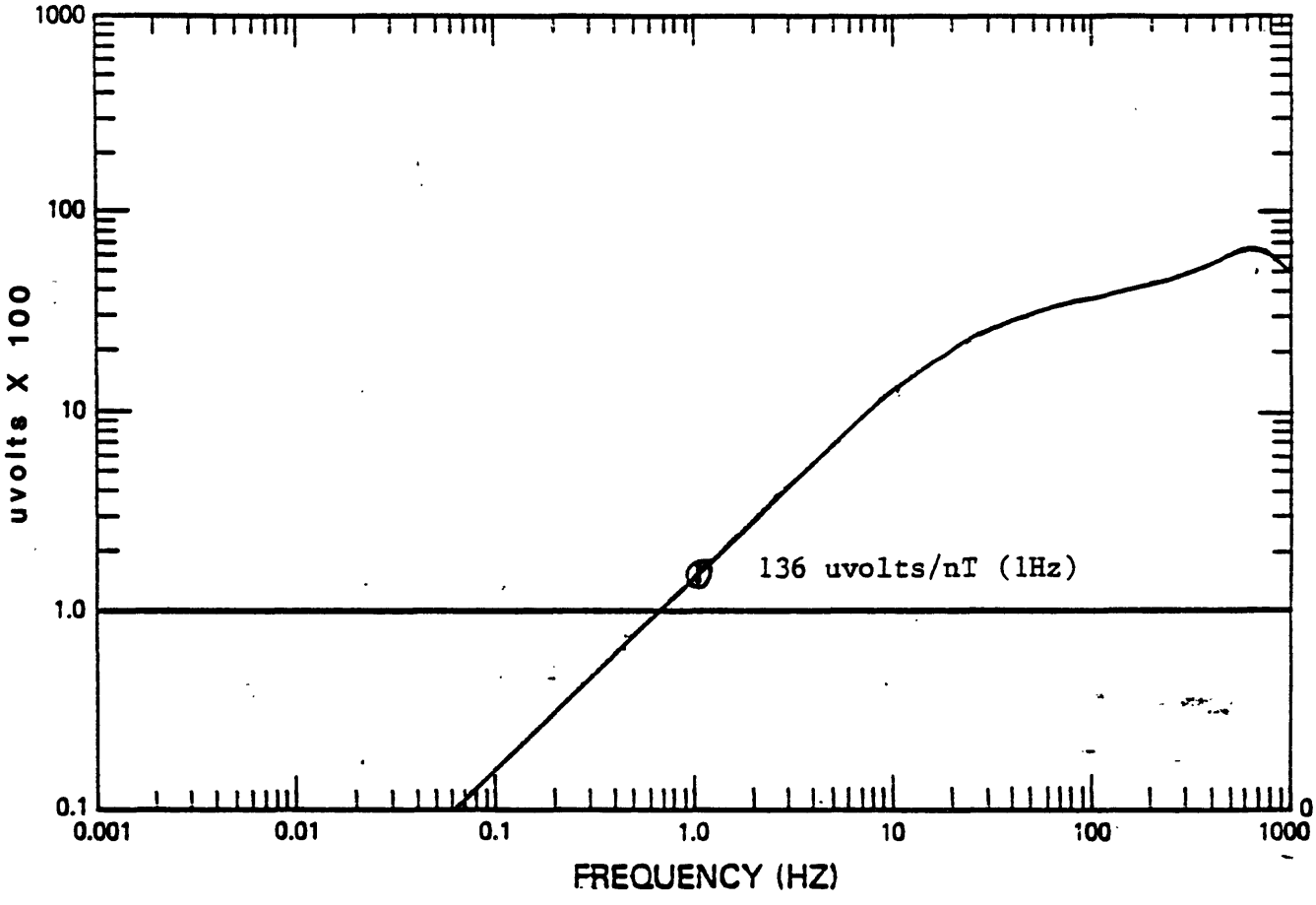

Figure 3.--Amplitude response of the 60 in induction coils.

Figure 4.--Photograph of aluminum arbor manufactured for mounting wire spools into a lathe for coil winding.

Figure 5.--Photograph of end of one of the wire spools and template for drilling five necessary holes in each end of spool as described in text.

Figure 6.--Manufactured collet for chucking the wound spools of wire into a lathe in order to facilitate boring out the spool centers.

Figure 7.--Aluminum clamp shown which positions the individual spools on the core tube.

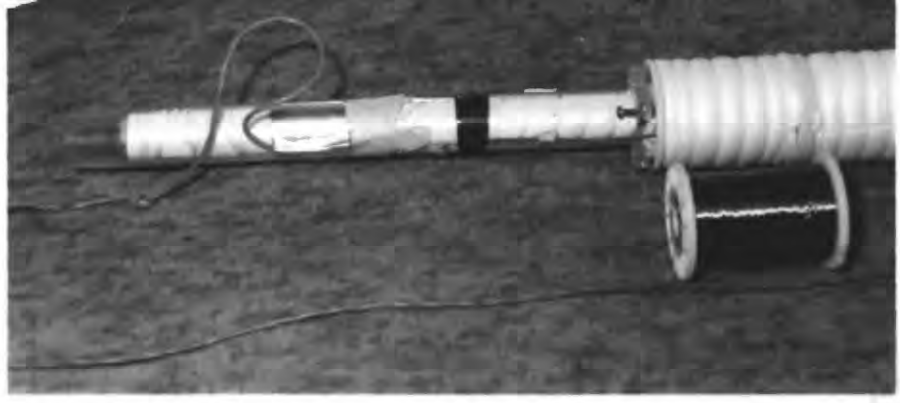

Figure 8.--High density foam installed on the spools to protect wire and secure winding-core assembly into outer housing.

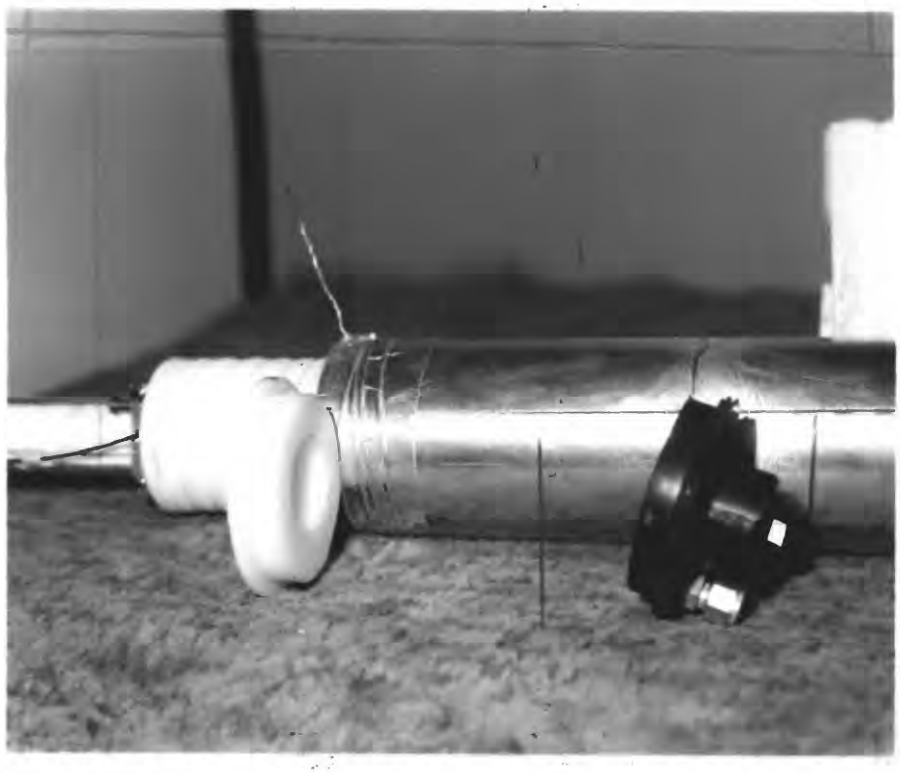

Figure 9.--End caps for the coil assembly, one of which was made from a 3.5 in diameter disk of nylon stock and the other of which was made from a standard plastic pipe plug.

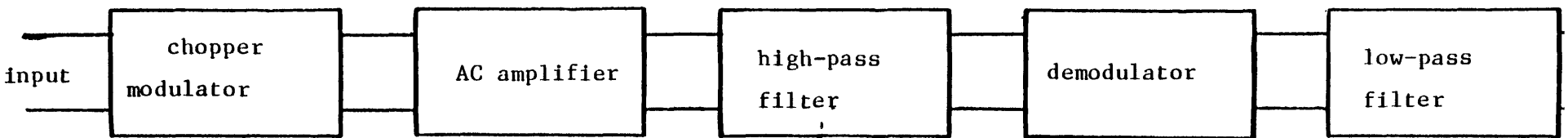

Figure 10.--Block diagram of the chopper amplifier.

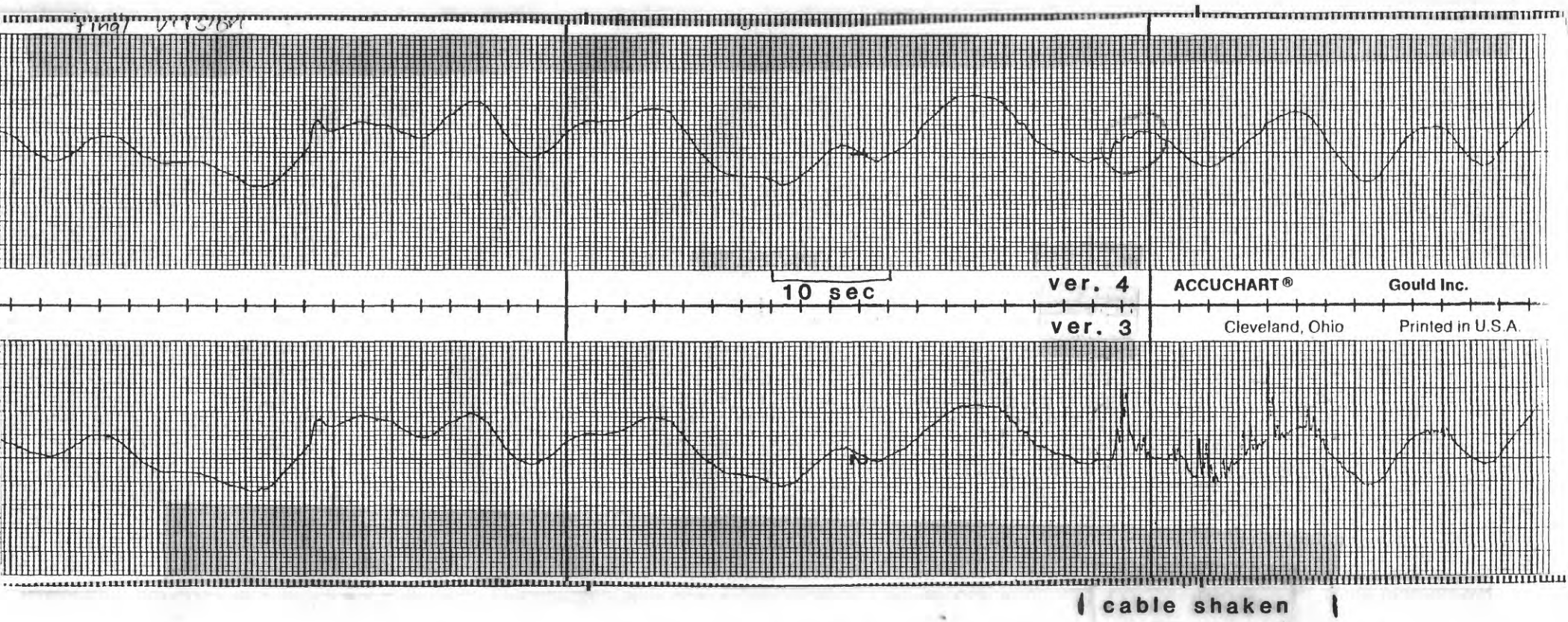

Figure 11.--Strip chart record showing the difference in noise generated by shaking the output trunk cable in a parallel coil-preamp system using version three (bottom) and version four (top) amplifiers.

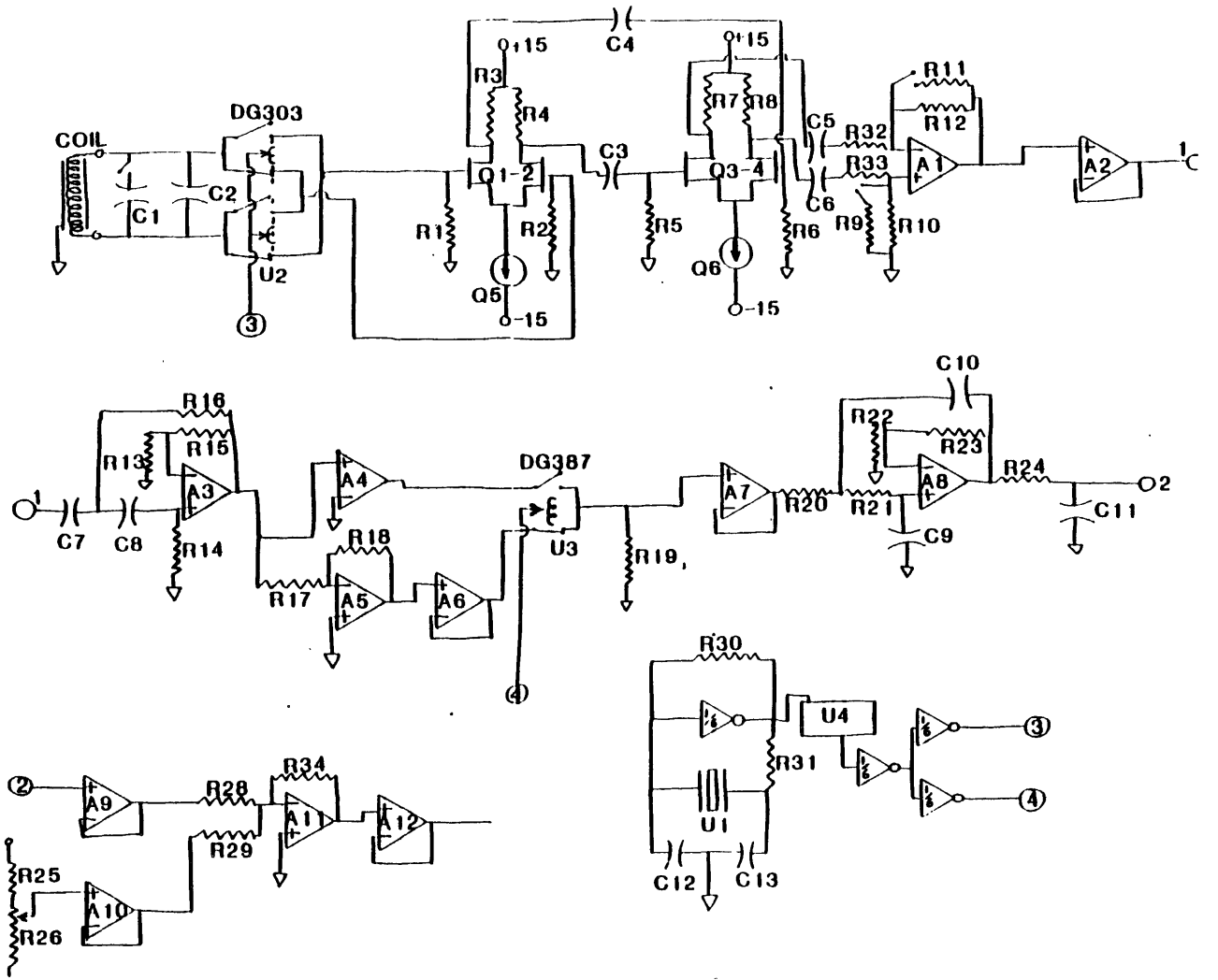

FIGURE 12a

Figure 12.--Schematic for the coil amplifier (a) symbolic ; (b) component value.

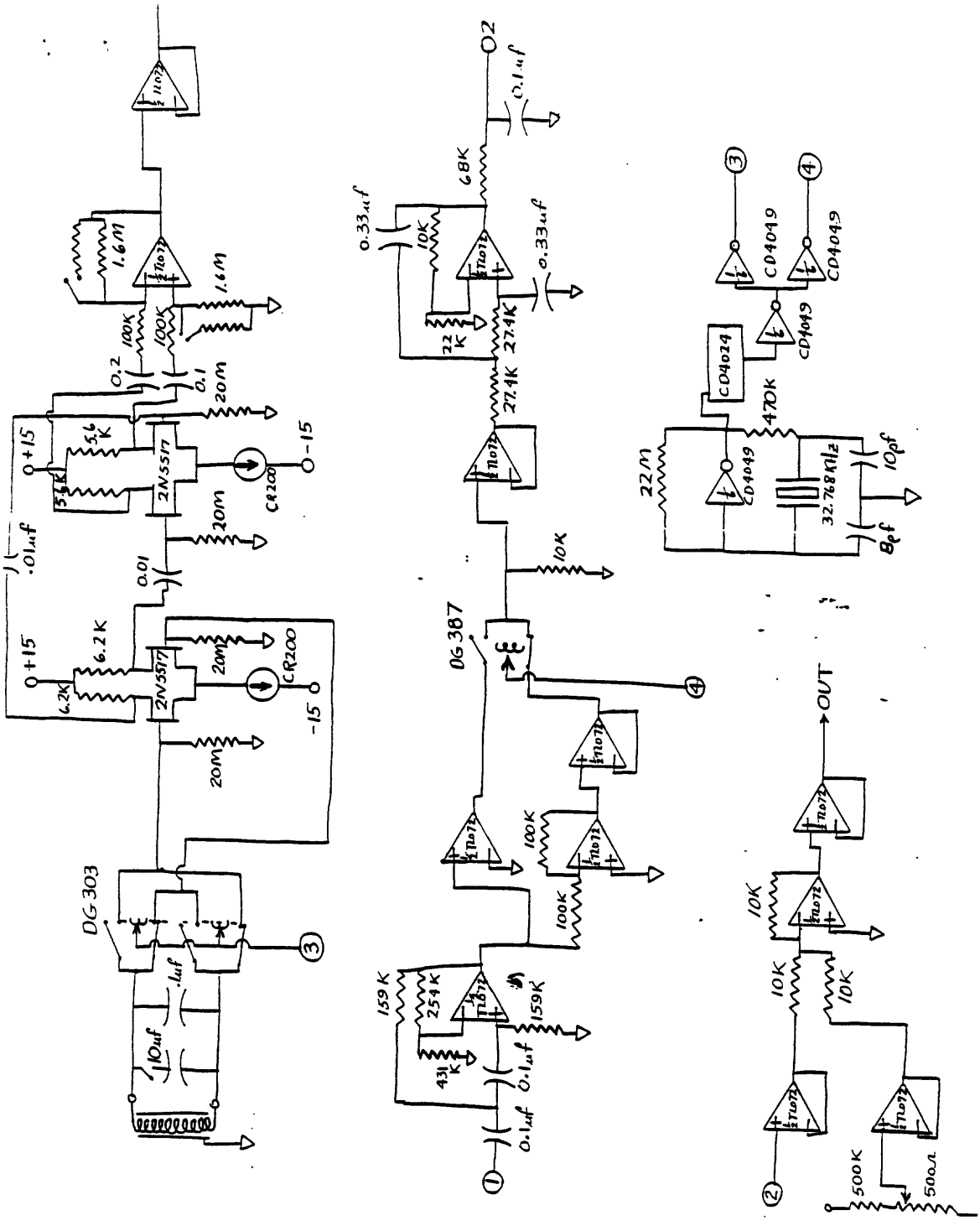
DG303
DG387
2N5517
CR200
TL072
CD4049
CD4024
OUT
32.768 KHz
500K

FIGURE 12b

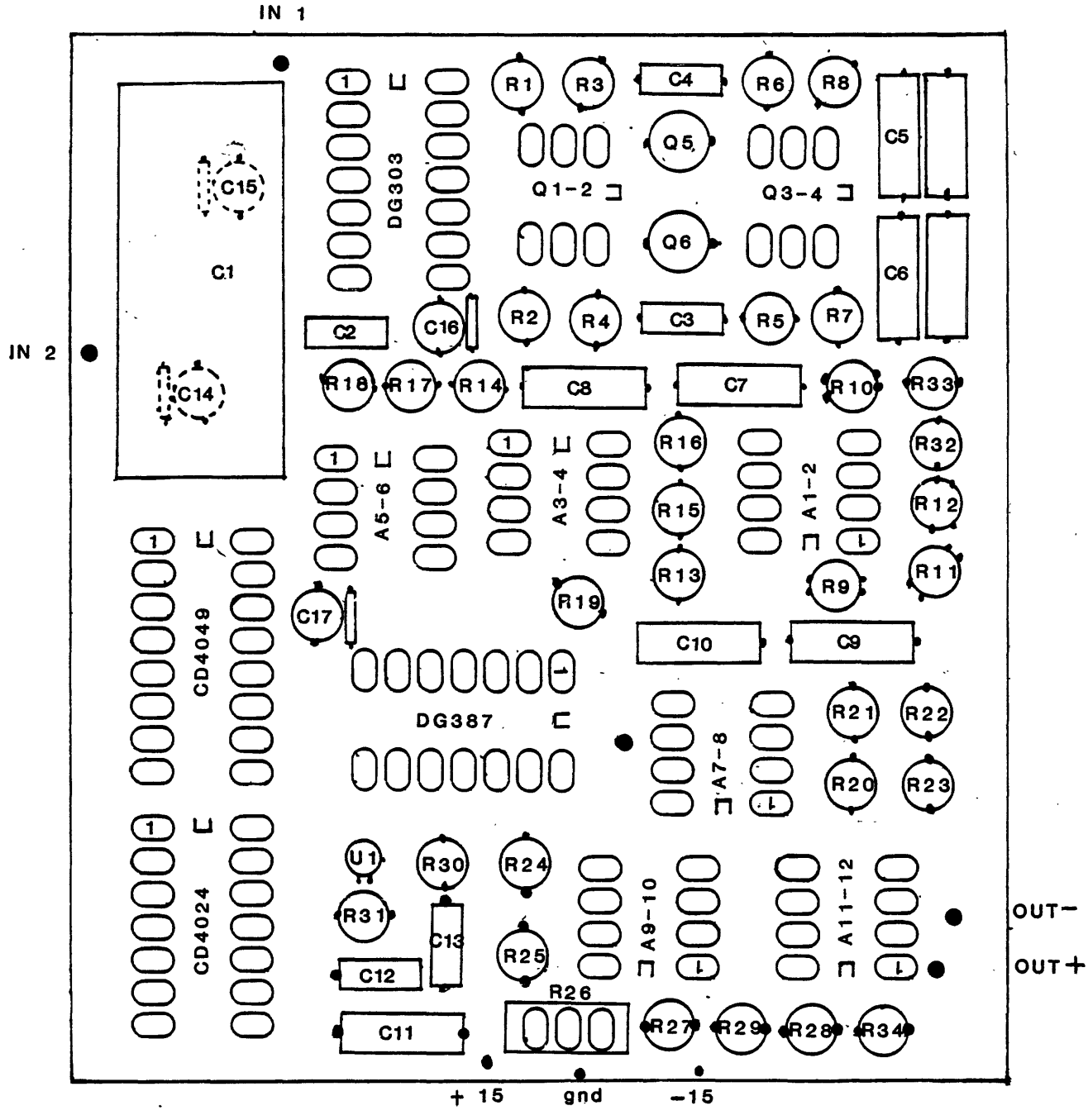

Figure 13.--Printed circuit board layout.

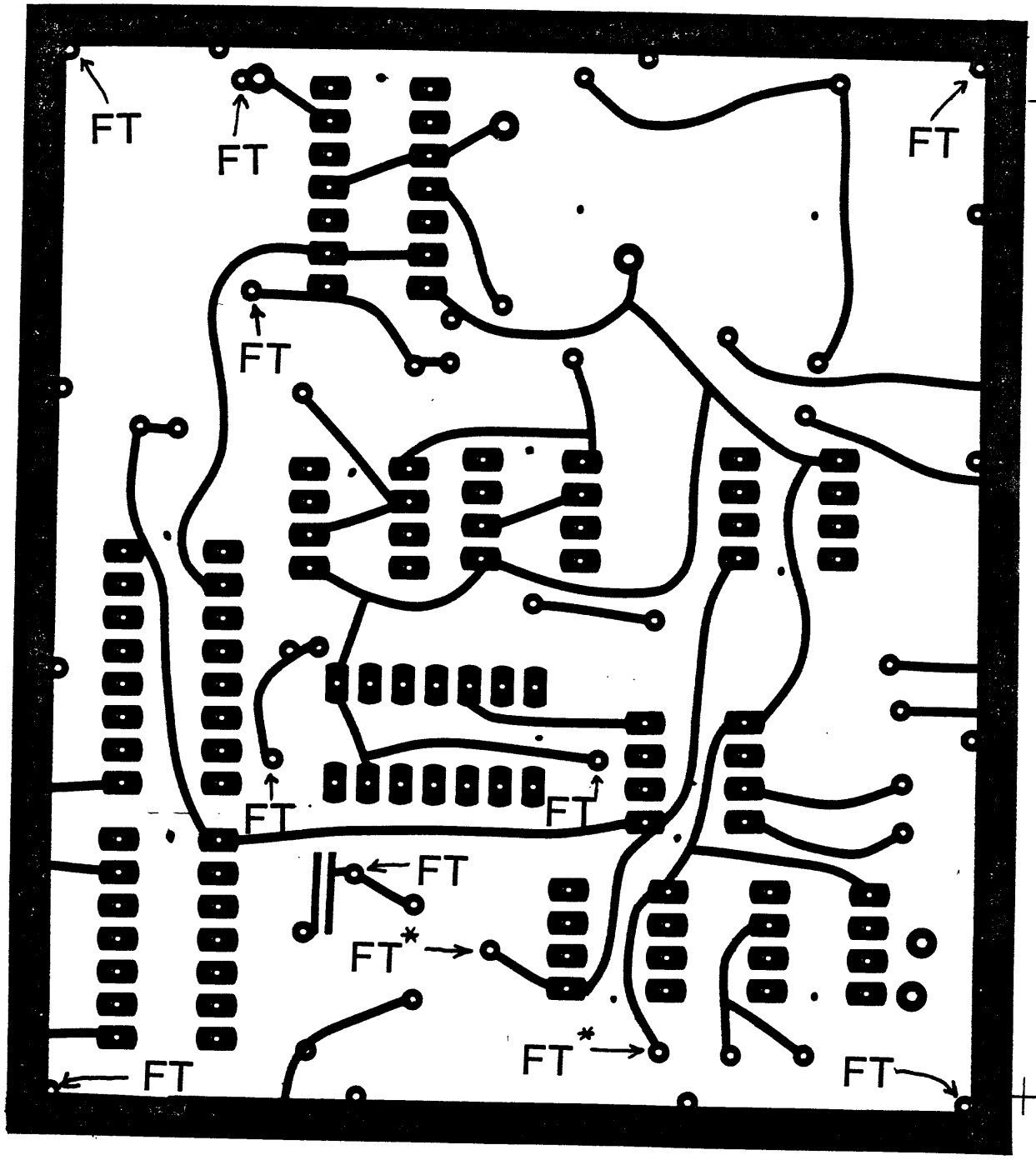

Figure 14.--PC board artwork composite, with feedthroughs required labeled FT.

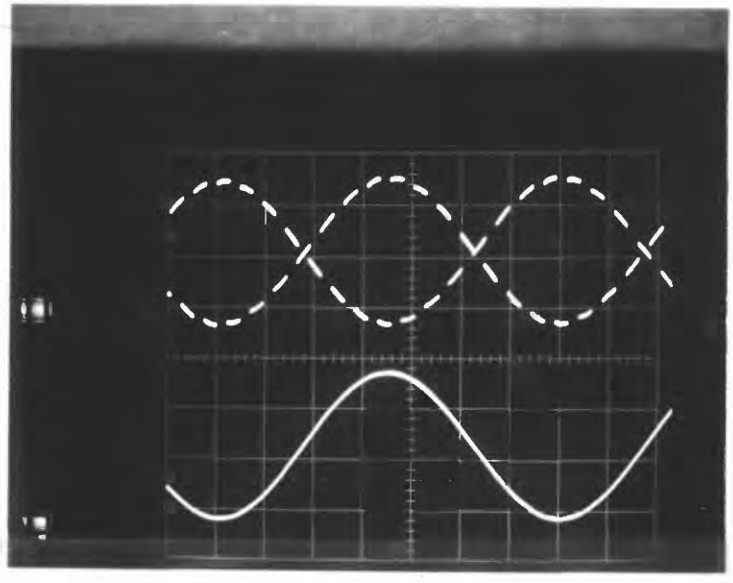

Figure 15.--Photo of sine-wave signal in amplifier at a point just prior to demodulator (upper) and overall output signal (lower).

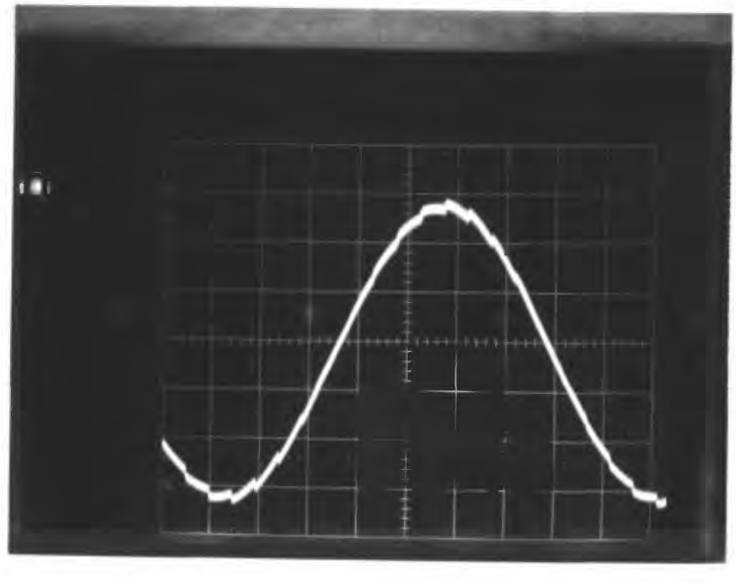

Figure 16.--Photo of output from demodulator of sine wave input.

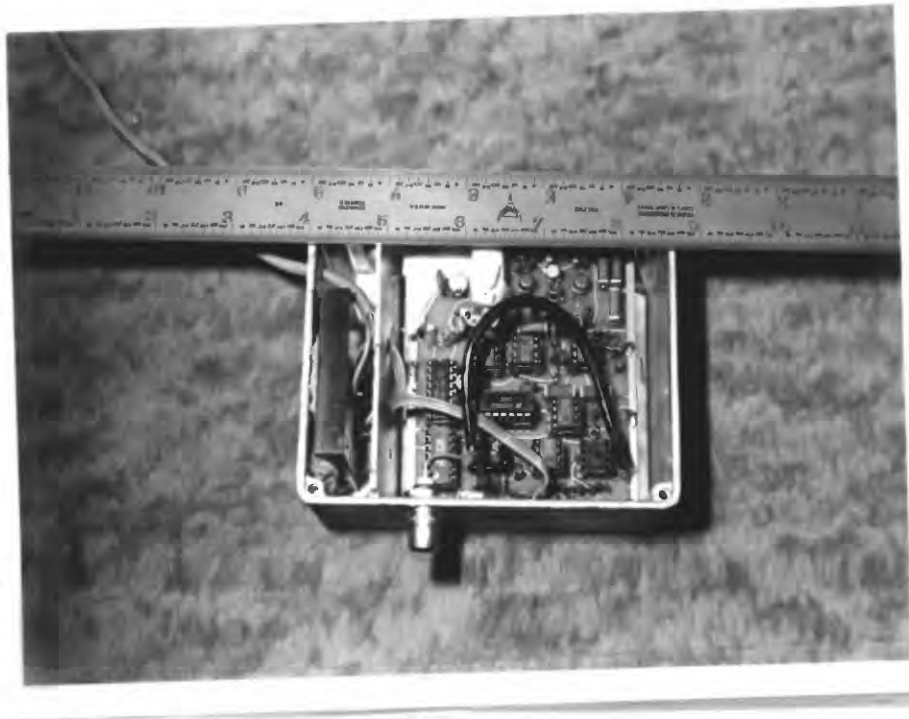

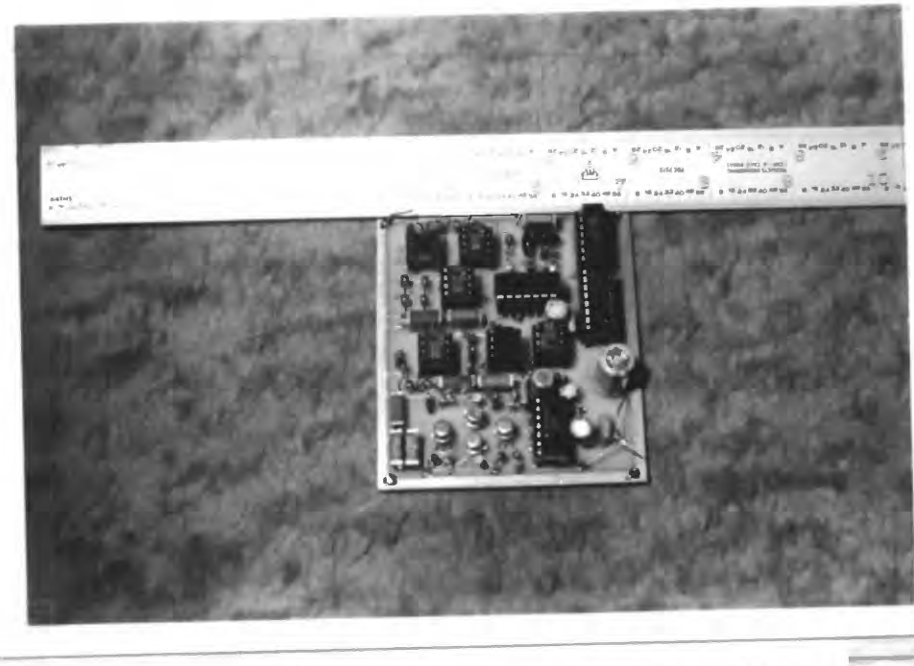

Figure 17.--Photos of completed amplifier.

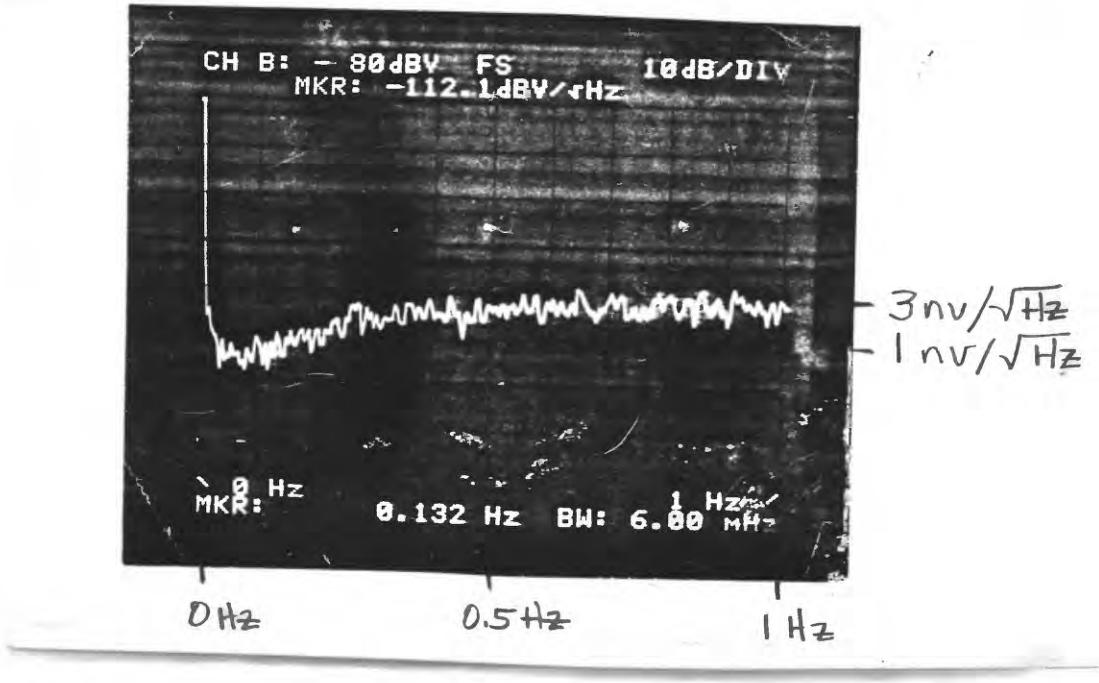

Figure 18.--Spectrum analyzer display, showing noise of coil amplifier with shorted input over frequency band from 0.1 to 1 Hz.

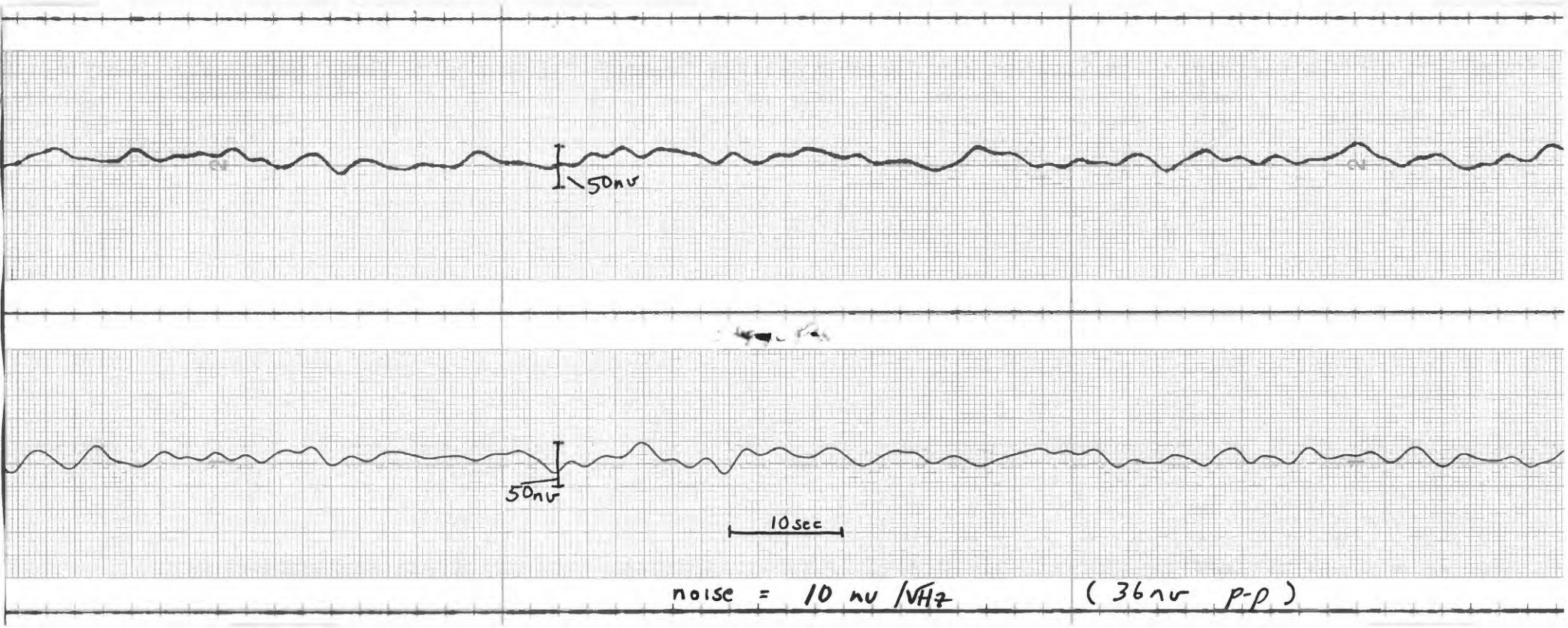

Figure 19.--Chart record of noise amplitude (time series) over frequency band from 0.005 to 0.2 Hz for two version four amplifiers.

Figure 20.--Overall coil-amplifier response as used in USGS MT system.